

AD-A053 025

COLORADO STATE UNIV FORT COLLINS DEPT OF CHEMISTRY

F/6 7/2

A LIGAND FIELD THEORY ANALYSIS OF THE SPECTRA OF THE T2G3 LEVEL--ETC(U)

MAR 78 J D WEBB, E R BERNSTEIN

N00014-75-C-1179

UNCLASSIFIED

TR-21

NL

| of |
AD
A053025



12
B.S.

OFFICE OF NAVAL RESEARCH
Contract N00014-75-C-1179
Task No. NR 056-607
TECHNICAL REPORT NO. 21

AD A 053025

"A LIGAND FIELD THEORY ANALYSIS OF THE SPECTRA
OF THE t_{2g}^3 LEVELS OF IrF_6 "

by

J. D. WEBB AND E. R. BERNSTEIN

Prepared for Publication in
Molecular Physics

Department of Chemistry
Colorado State University
Fort Collins, Colorado 80523

March 1978

DDC
RECEIVED
APR 24 1978
B

AD No. _____
DDC FILE COPY

Reproduction in whole or in part is permitted for
any purpose of the United States Government.

Approved for Public Release; Distribution Unlimited.

UNCLASSIFIED

SECURITY CLASSIFICATION OF THIS PAGE (When Data Entered)

REPORT DOCUMENTATION PAGE		READ INSTRUCTIONS BEFORE COMPLETING FORM	
1. REPORT NUMBER TR-21	2. GOVT ACCESSION NO.	3. RECIPIENT'S CATALOG NUMBER	
4. TITLE (and Subtitle) "A Ligand Field Theory Analysis of the Spectra of the t_{2g}^3 Levels of IrF_6 "		5. TYPE OF REPORT & PERIOD COVERED Technical Report	
7. AUTHOR(s) J. D. Webb and E. R. Bernstein		9. CONTRACT OR GRANT NUMBER(s) N00014-75-C-1179	
9. PERFORMING ORGANIZATION NAME AND ADDRESS Department of Chemistry Colorado State University Fort Collins, Colorado 80523		10. PROGRAM ELEMENT, PROJECT, TASK AREA & WORK UNIT NUMBERS NR 056-607	
11. CONTROLLING OFFICE NAME AND ADDRESS Office of Naval Research Arlington, VA 22217		12. REPORT DATE March 1978	
14. MONITORING AGENCY NAME & ADDRESS (if different from Controlling Office)		13. NUMBER OF PAGES 36 P.	
		15. SECURITY CLASS. (of this report) Unclassified	
		15a. DECLASSIFICATION/DOWNGRADING SCHEDULE	
16. DISTRIBUTION STATEMENT (of this Report) Approved for Public Release; Distribution Unlimited.			
17. DISTRIBUTION STATEMENT (of the abstract entered in Block 20, if different from Report)			
18. SUPPLEMENTARY NOTES			
19. KEY WORDS (Continue on reverse side if necessary and identify by block number) Crystal Field Theory Configuration Interaction $5d(t_{2g}^3)$ States Charge Transfer States			
20. ABSTRACT (Continue on reverse side if necessary and identify by block number) Calculations are presented for the t_{2g}^3 molecular levels of IrF_6 which indicate a substantial interaction with charge transfer levels at ca. 20,000 cm^{-1} . Interaction between charge transfer and t_{2g}^* states is so extensive that the			

DD FORM 1473 1 JAN 73

EDITION OF 1 NOV 65 IS OBSOLETE S/N 0102-014-6601

UNCLASSIFIED

SECURITY CLASSIFICATION OF THIS PAGE (When Data Entered)

404 992

hc

cm^{-1}
1/cm
ave

20. (continued...)

five t_{2g}^3 levels cannot be fit with physically reasonable Racah, spin orbit, and crystal field parameters. Parameter values presented are derived from a fit of the lowest three levels only: $B = 297 \text{ cm}^{-1}$; $C = 1167 \text{ cm}^{-1}$; $\zeta_{5d} = 4182 \text{ cm}^{-1}$ and $10 Dq = 35,000 \text{ cm}^{-1}$. Gas-to-crystal shifts and site splittings are then calculated that further indicate strong influence of charge transfer states on the nature of the t_{2g}^3 manifold. Finally, new data for the $\Gamma_{8g} (^2E_g)$ and $\Gamma_{6g} (^2T_{1g})$ states at $1.2 \mu\text{m}$ are given. Small Jahn-Teller interactions are observed in the $\Gamma_{8g} (^2E_g)$ state at this wavelength and a substantial site splitting is assigned for it. Both of these effects further demonstrate the importance of charge transfer admixture in the t_{2g} manifold.

ACCESSION for	
NTIS	White Section <input checked="" type="checkbox"/>
DDC	Buff Section <input type="checkbox"/>
UNANNOUNCED	<input type="checkbox"/>
JUSTIFICATION _____	
BY _____	
DISTRIBUTION/AVAILABILITY CODES	
Dist.	AVAIL. and/or SPECIAL
A	

I. INTRODUCTION

IrF_6 has played an important role in the ligand field theory of $5d^n$ transition metal compounds.¹⁻⁸ It is well established that the sharp, detailed spectra observed in the visible and near IR can be described approximately as transitions within a t_{2g}^3 manifold.^{2,9} However, a rigorous attempt to match observed and calculated^{6,10a,b} electronic energies has not been made. Present availability of definitive assignments of electronic origins in both vapor⁹ and mixed crystals of $\text{IrF}_6/\text{MoF}_6$ ^{11,12} makes a detailed ligand field theory study feasible. Additional mixed crystal data for the Γ_{8g} (2E_g) and Γ_{6g} (${}^2T_{1g}$) levels of IrF_6 are presented here to facilitate further comparison and complete the requisite data set.

There are several reasons why such a study might be useful. First, the most obvious benefit would be determination of reliable electrostatic (B, C) and spin-orbit (ζ_{5d}) parameters. Comparison with other members of the series (ReF_6 , OsF_6 , PtF_6) might then allow insight into the nature of ligand-metal interactions in these high oxidation state (VI) compounds. Second, the extent to which charge-transfer (CT) states interact with t_{2g}^n ligand field states is still an open question. In the case of CrBr_3 ($3d^3$), it has been speculated that such an interaction accounts for the inability to fit observed t_{2g}^3 levels with a ligand field calculation.¹³ If interaction with CT states is important, IrF_6 is a good candidate for study because an even CT state (Γ_{6g} or Γ_{7g}) has recently been identified only $\sim 1,000 \text{ cm}^{-1}$ above the Γ_{8g} (${}^2T_{2g}$) origin¹¹ at $-14,900 \text{ cm}^{-1}$ (the more intense odd CT bands begin at $-18,500 \text{ cm}^{-1}$). Third, since both vapor and mixed crystal data are available, gas-to-crystal shifts and site splittings can also be studied. These small electrostatic perturbations can be effectively employed to generate detailed information about the nature of the (nominally) t_{2g}^3

levels of IrF_6 . The magnitude, direction, and nature of the response of the electronic and vibronic states to crystal interactions will be a sensitive function of the actual state descriptions.

In Section IIIA, results of an attempt to fit observed t_{2g}^3 levels of IrF_6 with a parametric ligand field calculation are discussed. Gas-to-crystal shift data and low symmetry crystal field splitting of the Γ_{8g} levels are examined in Section IIIB and IIIC, respectively. Mixed crystal data for the Γ_{8g} (2E_g) and Γ_{6g} (${}^2T_{1g}$) levels of $\text{IrF}_6/\text{MoF}_6$ are discussed in detail in Section IIID.

II. METHODS AND RESULTS

A. Experimental

A summary of data and assignments for the Γ_{8g} (2E_g) and Γ_{6g} (${}^2T_{1g}$) levels of $\text{IrF}_6/\text{MoF}_6$ are given in Table 1. This table completes the $\text{IrF}_6/\text{MoF}_6$ mixed crystal data for t_{2g}^3 levels of IrF_6 .^{11,12} These spectra are also presented in Figures 1 and 2. Experimental methods employed are identical to those presented in reference 11.

B. Calculational

Results of an attempt to fit observed t_{2g}^3 ligand field levels of IrF_6 with a parametric calculation are given in Tables 2 and 3. The energy levels were calculated using Eisenstein's^{10a,b} d^3 energy matrices; however, due to the large ligand field splitting ($10 Dq \sim 35,000 \text{ cm}^{-1}$), only one set of Racah and spin-orbit parameters (B, C, ζ_{5d}) were used. A linear least squares routine was employed in parameter variation for an optimum fit. The results given in Table 2 were obtained by optimizing the fit of all five excited t_{2g}^3 levels while those in Table 3 were obtained by optimizing the fit of only the lowest three levels.

An attempt to calculate gas-to-crystal shifts for IrF_6 and ReF_6 (Tables 4 and 5) by varying the ligand field parameter Dq is summarized in Table 6. The IrF_6 $B, C,$ and ζ_{5d} parameters employed were those obtained for the calculation reported in Table 3. A spin-orbit parameter value of $3,200 \text{ cm}^{-1}$ was used for the ReF_6 gas-to-crystal shift calculations. A tetragonal crystal field calculation for a d^3 system was also carried out in order to evaluate site splitting mechanisms. Since appropriate matrix elements for a strong field-double group basis set are not available, these are given in Table 7. Tetragonal field matrix elements were generated by the appropriate basis transformation of Rahman's¹⁴ d^3 tetragonal matrix elements for a strong field-

single group basis. Transformed tetragonal matrix elements may then be combined with Runciman and Schroeder's⁶ octahedral d^3 matrices, since Tanabe and Sugano's phase is used throughout.¹⁵ An example of this calculation is given in Table 8. The appropriate one-electron tetragonal parameters ρ and μ are as follows:

$$\left. \begin{aligned} \langle t_{2g^z} | \hat{O}(e_g, \theta) | t_{2g^z} \rangle &= -\frac{2}{3} \rho \\ \langle t_{2g^x} | \hat{O}(e_g, \theta) | t_{2g^x} \rangle &= \langle t_{2g^y} | \hat{O}(e_g, \theta) | t_{2g^y} \rangle = \frac{1}{3} \rho \end{aligned} \right\} \quad (1)$$

$$\langle e_{g^{\theta}} | \hat{O}(e_g, \theta) | e_{g^{\theta}} \rangle = - \langle e_{g^{\epsilon}} | \hat{O}(e_g, \theta) | e_{g^{\epsilon}} \rangle = -\frac{1}{2} \mu \quad (2)$$

III. DISCUSSION

A. Calculations of t_{2g}^3 electronic levels of IrF_6

Results of IrF_6 calculations (Table 2) indicate several difficulties with the parametric fit of all the t_{2g}^3 levels. The main problem seems to be with the Racah parameters (e.g., $B(\text{IrF}_6) < 0$), although the low spin-orbit value ($\zeta_{5d}(\text{IrF}_6) = 3012 \text{ cm}^{-1}$) compared with that of ReF_6^4 ($\zeta_{5d} \sim 3200 \text{ cm}^{-1}$) and the large average absolute standard deviation ($\sigma \sim 250 \text{ cm}^{-1}$) are also disturbing. Note, however, that values obtained for the Racah parameters are not quite as poor as might appear at first glance since only $3B + C$ is determined directly within the t_{2g}^3 block. The unphysical negative value for B and the resulting high value for C do, however, indicate that the t_{2g}^3 levels are perturbed.

A possible cause of the above difficulties might be thought to be neglect of the Trees' correction, which is important for 3d transition metal ions¹³. The calculation for ReF_6^{-2} in Table 2, however, demonstrates that such is not the case for these 5d systems.

The most plausible explanation for the above perturbation is a substantial interaction between the charge-transfer (CT) and ligand field electronic states. If this is the case, one expects that ligand field calculations for ReF_6^{-2} t_{2g}^3 states will be more accurate than those for ReCl_6^{-2} and IrF_6 (see Table 2) due to the proximity of the CT and upper t_{2g}^3 states in the latter two systems (see Table 9). Since only the mixing of even CT states into the $5d-t_{2g}^3$ manifold is expected to be important in this context, this correlation requires that a rough equality exists between the onset energies of even and odd CT states in the two ionic systems. This is found to be the case for IrF_6 .¹¹

Another calculation can be done which indicates more directly that CT states do indeed perturb and mix with the t_{2g}^3 manifold. Ligand field para-

parameters in this calculation are optimized to fit only the lowest three excited levels (Table 3), as it is expected that these levels are less perturbed by CT bands. This type of calculation for IrF_6 (Table 3) supports the CT hypothesis in that the resulting parameters ($\zeta_{5d} = 4000 \text{ cm}^{-1}$, $\frac{C}{B} = 4$), are more reasonable than those obtained for the fit of all five IrF_6 levels ($\zeta_{5d} = 3000 \text{ cm}^{-1}$, $\frac{C}{B} = 15$). Of course, calculated energies for the Γ_{7g} (${}^2T_{2g}$) and Γ_{8g} (${}^2T_{2g}$) levels are much higher than those observed. The analogous calculations for ReF_6^{-2} and ReCl_6^{-2} yield results expected in this theory: the Γ_7 (${}^2T_{2g}$) and Γ_8 (${}^2T_{2g}$) calculated levels for ReCl_6^{-2} are far from the observed, while those for ReF_6^{-2} are substantially closer.

These considerations all lead to the conclusion that there is a substantial interaction between even CT and t_{2g}^3 ligand field electronic levels of an isolated gas phase (O_h^*) IrF_6 molecule. It is expected that similar interactions exist in other hexahalides with low-lying CT bands (i.e., ReCl_6^{-2} , ReBr_6^{-2} , PtF_6 , and OsF_6).

In view of the magnitude of the shifts of the Γ_{7g} (${}^2T_{2g}$) and Γ_{8g} (${}^2T_{2g}$) levels of IrF_6 , it is reasonable to assume that the lower levels are also significantly shifted, and thus that the parameter values obtained for IrF_6 in Table 3 are only approximate. It may be said, however, that the present spin-orbit parameter value ($\zeta_{5d} = 4182 \text{ cm}^{-1}$) is more realistic than that derived by Jorgensen⁸ ($\zeta_{5d} = 3100 \text{ cm}^{-1}$) who based his estimate on the energies of the Γ_{7g} (${}^2T_{2g}$) and Γ_{8g} (${}^2T_{2g}$) levels of IrF_6 .

B. Gas-to-crystal shifts of the t_{2g}^3 levels of IrF_6

The gas-to-crystal (GC) shift data for mixed crystals of IrF_6 in UF_6 , WF_6 , and MoF_6 are presented in Tables 4a and 5a; analogous data for ReF_6 are given in Tables 4b and 5b. The IrF_6 mixed crystal data have two notable features:

GC shifts of the lowest three electronic levels are virtually equal in each host (Table 4a), and the normalized (to the smallest shift in each host) sets of shifts are nearly equal in the three hosts (see Table 5). The shifts themselves appear to be linearly dependent on a single quantity which is varying from host to host. Note that the ReF_6 GC shifts are nearly two orders of magnitude smaller than those found for IrF_6 .

The crystal field (to be distinguished from ligand field) which acts on an IrF_6 molecule at a crystal site is a reasonable candidate for the cause of GC shifts. Thus, the form of the crystal field operator and its effect on various approximate IrF_6 wavefunctions will be examined. Site symmetry of all hexafluoride crystals (except 295 K neat IrF_6) employed in this study is $C_s (\sigma_d)$.¹¹ Since IrF_6 is octahedral in the gas phase, the crystal field operator which acts on the t_{2g} electrons of IrF_6 may be expressed in terms of O_h^* tensor operators¹⁶ as follows:

$$\hat{O}(\text{CF}) = \hat{O}(\text{octahedral}) + \hat{O}(\text{tetragonal}) + \hat{O}(\text{trigonal}) + \hat{O}'(t_{2g}, \zeta) + \{\hat{O}(t_{1g}, x) - \hat{O}(t_{1g}, y)\} + \hat{O}(\text{ungerade terms}) \quad (3)$$

in which

$$\hat{O}(\text{octahedral}) = \hat{O}(a_{1g})$$

$$\hat{O}(\text{tetragonal}) = \hat{O}(e_g, \theta)$$

$$\hat{O}(\text{trigonal}) = \{\hat{O}(t_{2g}, \xi) + \hat{O}(t_{2g}, \eta) + \hat{O}(t_{2g}, \zeta)\}$$

and $\hat{O}'(t_{2g}, \zeta)$ is needed to maintain rigorous C_s^* site symmetry. Gerade terms are given in detail since they are typically the more important; ungerade terms are usually important only in intensity considerations.¹⁶

The 295 K neat IrF_6 crystal GC shift data (Table 5) provide evidence necessary for the determination of the relative importance of each of the terms in Equation 3. Above -273 K all second and third row transition metal hexa-

fluoride crystals exhibit a body-centered cubic modification.¹⁷ More detailed crystal structure data on MoF_6 ¹⁸ imply that in the cubic modification, hexafluoride molecules are undistorted from an octahedral configuration. This argues that non-totally symmetric terms in the crystal field are not of major importance in the cubic crystal. Nonetheless the GC shifts observed in 295 K neat IrF_6 crystals are substantial, about 50% of the shift observed at 2 K.

The conclusion which may be drawn from the above physical arguments is that the totally-symmetric crystal field operator $\hat{O}(a_{1g})$ is probably the dominant one for these considerations. Moreover, it may be shown that none of the non-totally symmetric terms may lead to diagonal matrix elements which could cause an overall GC shift. Non-totally symmetric operators will thereby cause a GC shift only through off-diagonal matrix elements involving sizeable energy denominators. Consequently, subsequent discussion will consider only the effect of $\hat{O}(a_{1g})$.

The GC shifts calculated with the $\hat{O}(a_{1g})$ operator depend critically on the functions chosen to represent the ligand field states. The first approximate wavefunctions of IrF_6 which will be considered are those involving only t_{2g}^3 functions (i.e., all configuration interaction is neglected). If the secular matrix for the octahedral crystal field operator is formed with these functions, it is found to be diagonal with each diagonal element equal to $-4Dq'$; thus, at this level of approximation no GC shift occurs.

If complete ligand field wavefunctions are considered (i.e., e_g configuration interaction included) then, as illustrated in Table 6, GC shifts are predicted. However, this mechanism can be rejected for three reasons: the increase in the octahedral field necessary to produce shifts of the magnitude

observed is larger than what is reasonable ($10 Dq' \sim 15,000 \text{ cm}^{-1}$); calculated shifts do not match the observed GC shifts well; and concomitant GC shifts in ReF_6 are not observed.

Considerations in Section IIA led to the conclusion that in gas phase IrF_6 , t_{2g}^3 levels are perturbed by nearby even charge-transfer (CT) bands; CT character is thereby mixed into these ligand field free molecule wavefunctions. The final approximate wavefunctions considered are these ligand field-CT functions. The GC shift data may be explained if sufficient CT character is present in the above functions to cause diagonal $\hat{O}(a_{1g})$ matrix elements to deviate substantially from the $-4 Dq'$ value mentioned above. However, since there is not an adequate theory which would allow a quantitative assessment of this mechanism, only qualitative remarks are possible. Three points favoring this interpretation are:

- 1) The highest two t_{2g}^3 levels of IrF_6 have been strongly repelled by CT bands (~ 1900 and $\sim 600 \text{ cm}^{-1}$, Table 3). Presumably, the lower three levels are also repelled, both by CT bands and by perturbed Γ_{7g} (${}^2T_{2g}$) and Γ_{8g} (${}^2T_{2g}$) levels. The magnitudes of level repulsions imply substantial mixing of t_{2g}^3 and CT wavefunctions.
- 2) The magnitude of the GC shifts is largest for the Γ_{8g} (${}^2T_{2g}$) and Γ_{7g} (${}^2T_{2g}$) levels which are energetically closest to the CT bands.
- 3) The linear behavior of GC shifts with host-to-host variation noted above (see Table 5) agrees with the simple energy expressions implied by this mechanism. These energy expressions depend linearly on an octahedral crystal field parameter which is expected to evidence small variations as a function of host.

On the other hand, the proposed CT- t_{2g}^n mixing mechanism for GC shifts does not appear to be supported by ReF_6 GC shift data (Table 5b). The ReF_6 GC shifts are not as large as might be expected based on standard second-order perturbation theory and comparison with the GC shift for the IrF_6 Γ_{8g} (${}^2T_{1g}$) level considering the energies of the respective CT bands (Table 9). It is however, difficult to comment on this apparent lack of agreement; there are too many unknown quantities involved. Little is known about the detailed nature of the interaction between CT and ligand field states and how the interaction might change from IrF_6 to ReF_6 . Thus, in spite of this point, the CT-admixture mechanism constitutes a reasonable interpretation of the GC shift data.

C. Low symmetry crystal field splitting of the $t_{2g}^3 \Gamma_{8g}$ levels of IrF_6

Site splittings of the electronic origins of $t_{2g}^3 \Gamma_{8g}$ levels of IrF_6 in various host crystals are given in Table 10. In contrast to the situation outlined in Section IIIB, non-totally symmetric crystal field operators in Equation 3 are important for this effect. Calculations of site splitting associated with a general low symmetry crystal field (Equation 3) are prohibitively difficult because of the large number of parameters involved. However, it has been demonstrated by crystal structure (UF_6)¹⁹ and spectroscopic (MoF_6)¹¹ data that the (e_g, θ) tetragonal component of the field is probably a reasonable approximation to the field experienced by IrF_6 at host sites. The tetragonal crystal field matrix elements for a complete ligand field basis given in Table 7 were employed in this analysis. Results of this calculation are given in Table 8 and may be compared with experimental data in Table 10. The observed and calculated splitting of the Γ_{8g} (2E_g) level are found to be not even in qualitative agreement. In light of preceding discussion, this discrepancy may be interpreted in terms of CT-admixture

into the t_{2g}^3 levels. Clearly both t_{2g}^3 and charge-transfer states contribute to the observed splittings throughout the manifold. A detailed decomposition of the effects of CT-admixture, tetragonal crystal field, and their interplay with the Jahn-Teller interaction is not apparent at present. However, this subject is treated to some extent in reference 20.

D. Absorption spectra of the Γ_{8g} (2E_g) and Γ_{6g} (${}^2T_{1g}$) levels of $\text{IrF}_6/\text{MoF}_6$

Existence of a substantial site splitting of the Γ_{8g} (2E_g) level at 8200 cm^{-1} was important for the assessment of crystal field charge-transfer effects on IrF_6 Γ_{8g} states (Section IIIC). Since assignment of a 30.6 cm^{-1} site splitting of this level is not entirely obvious from the origin spectrum presented in Figure 1, it is necessary to indicate how this determination is made. Such an assignment becomes evident from an examination of the bending region (Figure 2 and Table 1) in which ν_6 and ν_4 are seen to have equally intense components separated by roughly 30 cm^{-1} . It should be noted that observation of crystal field splitting of the level at -8200 cm^{-1} provides the first strong evidence that the assignment of the level as Γ_{8g} (2E_g) is correct. Previous arguments were based on the observation of one component of the ν_2 (e_g) vibration and the supposition that its change in energy from that observed in the ground state is due to a Jahn-Teller interaction.⁹

The linewidths, especially of the origins and ν_6 , are larger than is typical for the rest of the t_{2g}^3 manifold. This may be due to the proximity of Γ_{8g} (2E_g) and Γ_{6g} (${}^2T_{1g}$) levels to the Γ_{8g} (${}^2T_{1g}$) level at $1.6 \mu\text{m}$. Vibronic coupling between these states could lead to fast relaxation which would broaden the transitions.

Broad lines and overlap of the Γ_{8g} (2E_g) and Γ_{6g} (${}^2T_{1g}$) manifolds have inhibited interpretation of the vibronic portion of the spectrum. Nonetheless, a weak Jahn-Teller interaction ($D_5 = 0.03$)¹¹ may be identified for the ν_5 (t_{2g}) vibration in the Γ_{8g} (2E_g) electronic manifold (see Figure 2 and Table 1).

IV. CONCLUSIONS

The main conclusion which may be drawn from this investigation is that the interaction of even charge-transfer (CT) bands with the t_{2g}^3 levels of free molecule IrF_6 is sufficiently strong to effect their detailed behavior. The following appear to be manifestations of the admixture of CT character into the t_{2g}^3 levels:

- 1) Failure of ligand field theory to give a reasonable parametric fit to all of the observed gas-phase t_{2g}^3 energies.
- 2) Substantial gas-to-crystal shifts for the t_{2g}^3 levels.
- 3) Tetragonal crystal field splitting of the $\Gamma_{8g} ({}^2E_g)$ level.

In spite of the CT interaction, rough ligand field theory parameters (B, C, ζ_{5d}) have been determined based on the lower three excited t_{2g}^3 levels (Table 3). It is found that the spin-orbit parameter is larger than previously believed.

Conclusive evidence for the assignment of the $\Gamma_{8g} ({}^2E_g)$ level of IrF_6 is found, based on site splitting of the origin. A small linear JT interaction has been identified in this state for the ν_5 mode ($D_5 \sim 0.03$).

REFERENCES

1. C. K. Jorgensen, *Acta Chem. Scand.* 12, 1539 (1958).
2. W. Moffitt, G. L. Goodman, M. Fred, B. Weinstock, *Mol. Phys.* 2, 109 (1959).
3. C. K. Jorgensen, *Mol. Phys.* 3, 201 (1960).
4. J. C. Eisenstein, *J. Chem. Phys.* 33, 1530 (1960).
5. B. N. Figgis, J. Lewis, F. E. Mabbs, *J. Chem. Soc.* 1961, 3138 (1961).
6. W. A. Runciman, K. A. Schroeder, *Proc. Roy. Soc. (London)* A265, 489 (1962).
7. C. K. Jorgensen, *Adv. Chem. Phys.* V, 33 (1963).
8. C. K. Jorgensen, *Z. Naturforschg.* 20a, 65 (1965).
9. J. C. D. Brand, G. L. Goodman, B. Weinstock, *J. Mol. Spec.* 37, 464 (1971).
10. a) J. C. Eisenstein, *J. Chem. Phys.* 34, 1628 (1960).
b) J. C. Eisenstein, *J. Chem. Phys.* 35, 2246 (1961).
11. E. R. Bernstein, J. D. Webb, *Mol. Phys.*, in press.
12. E. R. Bernstein, J. D. Webb, *Mol. Phys.*, in press.
13. J. Ferguson, D. L. Wood, *Austral. J. Chem.* 23, 861 (1970).
14. H. U. Rahman, *Physica* 53, 256 (1971).
15. Y. Tanabe, S. Sugano, *J. Phys. Soc. Japan* 9, 753 (1954).
16. S. Sugano, Y. Tanabe, H. Kamimura, "Multiplets of Transition-Metal Ions in Crystals," (Academic Press, NY, 1970).
17. S. Siegel, D. A. Northrop, *Inorg. Chem.* 5, 2187 (1966).
18. J. H. Levy, D. L. Sanger, J. C. Taylor, P. W. Wilson, *Acta Cryst.* B31, 1065 (1974).
19. J. C. Taylor, P. W. Wilson, J. W. Kelly, *Acta Cryst.* B29, 7 (1973).
20. G. R. Meredith, J. D. Webb, E. R. Bernstein, *Mol. Phys.* 34, 995 (1977).

Table 1. The absorption spectra of the Γ_{8g} (2E_g) and Γ_{6g} (${}^2T_{1g}$) levels of $\text{IrF}_6/\text{MoF}_6$ at 1.6 K with 1 cm^{-1} slitwidths. The accuracy is approximately $\pm 0.5 \text{ cm}^{-1}$.

λ_{Air} (\AA)	σ_{Vacuum} (cm^{-1})	I (a)	FWHH (b)	$\Delta\sigma_1$ (cm^{-1}) (c)	$\Delta\sigma_2$ (cm^{-1}) (d)	Assignments
12218.9	8181.8	M	10	0		Origin(a) $\{\Gamma_{8g}({}^2E_g)\}$
12173.3	8212.4	W	7	30.6		Origin(b) $\{\Gamma_{8g}({}^2E_g)\}$
11908.2	8395.3	M	16	213.5		ν_6 (a) $\{\Gamma_{8g}({}^2E_g)\}$
11869.5	8422.6	-	18	240.8		ν_5 ($J_5=3/2$) $\{\Gamma_{8g}({}^2E_g)\}$
11862.5	8427.6	M		245.8		ν_6 (b) $\{\Gamma_{8g}({}^2E_g)\}$
11814.5	8461.9	W	16	280.1		ν_5 ($J_5=1/2$) $\{\Gamma_{8g}({}^2E_g)\}$
11808.9	8465.9	M		284.1		ν_4 (a) $\{\Gamma_{8g}({}^2E_g)\}$
11767.3	8495.8	M	13	314.0		ν_4 (b) $\{\Gamma_{8g}({}^2E_g)\}$
11460.9	8722.9	M	12	541.1	0	Origin $\{\Gamma_{6g}({}^2T_{1g})\}$
11394.4	8773.8	W		592.1	51.0	Phonons $\{\Gamma_{6g}({}^2T_{1g})\}$
11295.7	8850.5	W	7	668.7	127.6	ν_2 $\{\Gamma_{8g}({}^2E_g)\}$ (?)
11206.5	8920.9	W		739.2	198.1	
11182.7	8939.9	S	21	758.1	217.0	ν_6 $\{\Gamma_{6g}({}^2T_{1g})\}$
11164.5	8954.5	M		772.7	231.6	
11121.3	8989.3	M		807.5	266.4	ν_5 $\{\Gamma_{6g}({}^2T_{1g})\}$
11105.8	9001.8	S		820.0	278.9	ν_4 $\{\Gamma_{6g}({}^2T_{1g})\}$
11081.3	9021.7	W		839.9	298.8	
11039.3	9056.1	W		874.3	333.2	$(\nu_2 + \nu_6)$ (a) $\{\Gamma_{8g}({}^2E_g)\}$ (?)

continued...

Table 1. (continued)

$\lambda_{\text{Air}}(\text{\AA})$	$\sigma_{\text{Vacuum}}(\text{cm}^{-1})$	I (a)	FWHH (b)	$\Delta\sigma_1(\text{cm}^{-1})$ (c)	$\Delta\sigma_2(\text{cm}^{-1})$ (d)	Assignments
10957.4	9123.8	W		941.9	400.8	$(\nu_2 + \nu_4)$ (a) $\{\Gamma_{8g}({}^2E_g)\}$ (?)
10859.3	9206.2	W		1024.4	483.3	$(\nu_5 + \nu_6)$ $\{\Gamma_{6g}({}^2T_{1g})\}$
10789.9	9265.4	W		1083.6	542.5	$(\nu_5 + \nu_4)$ $\{\Gamma_{6g}({}^2T_{1g})\}$
10612.1	9420.6	W		1238.8	697.7	ν_3 $\{\Gamma_{6g}({}^2T_{1g})\}$

a) Intensity: S = strong, M = medium, W = weak.

b) FWHH = full width at half-height.

c) Energy (cm^{-1}) relative to the $\Gamma_{8g}({}^2E_g)$ origin (a).

d) Energy (cm^{-1}) relative to the $\Gamma_{6g}({}^2T_{1g})$ origin.

Table 2. Comparison of ligand field calculations of the t_{2g}^3 levels of some $5d^3$ systems (IrF_6 , ReF_6^{-2} , ReCl_6^{-2}). Eisenstein's^(a) energy matrix for d^3 was used along with a linear least squares fitting routine which optimized the fit for all five levels. B and C are Racah's electrostatic parameters, ζ_{5d} is the spin-orbit coupling parameter, and $10 Dq$ is the ligand field parameter. Only B, C, ζ_{5d} were varied. The various Γ_{ig} label the t_{2g}^3 levels. All the values are given in wavenumbers.

a) IrF_6 (Vapor)	$\Gamma_{8g}(^2T_{1g})$	$\Gamma_{8g}(^2E_g)$	$\Gamma_{6g}(^2T_{1g})$	$\Gamma_{7g}(^2T_{2g})$	$\Gamma_{8g}(^2T_{2g})$
Observed: ^(b)	6261	8333	8858	12328	15156
Calculated:	6561	8397	8180	12345	15344

Parameters: $B = -221$, $C = 3188$, $\zeta_{5d} = 3012$, $10 Dq = 35000$ ^(c), $3B + C = 2525$.
Avg. Abs. Deviation^(g): 250.

b) ReF_6^{-2}					
Observed:	9080 ^(b)	10130 ^(b)	11160 ^(b)	17390 ^(d)	18670 ^(d)
Calculated:	9033	10278	11197	17329	18641

Parameters: $B = 665$, $C = 1504$, $\zeta_{5d} = 3019$, $10 Dq = 33100$ ^(e), $3B + C = 3499$.
Avg. Abs. Deviation: 64.

c) ReCl_6^{-2}					
Observed: ^(f)	7600 ^(b)	8906	9344	13840	15298
Calculated:	7748	8839	8844	13952	15443

Parameters: $B = 4$, $C = 2820$, $\zeta_{5d} = 2254$, $10 Dq = 30347$ ^(f), $3B + C = 2832$.
Avg. Abs. Deviation: 194.

- a) References 10a, b.
 b) Reference 9.
 c) The $10 Dq$ value of 35000 cm^{-1} was chosen on the basis of ReF_6^{-2} data^(d), ReF_6 data⁽²⁾, and expected trends. The results are not very sensitive to the value of this parameter.
 d) J. A. LoMenzo, S. Strobridge, H. H. Patterson, J. Mol. Spec. 66, 150 (1977).
 e) The $10 Dq$ value used is taken from ref. d. The parameter values for B, C, ζ found here are probably less realistic than those in ref. d since their data on the $^4T_{2g}$ levels was utilized. However, this calculation is for comparison purposes with the IrF_6 calculation only.
 f) P. B. Dorain, R. G. Wheeler, J. Chem. Phys. 45, 1172 (1966).
 g) Average Absolute Deviation of the calculated energies from the observed energies.

Table 3. Comparison of the ligand field calculations of the t_{2g}^3 levels of some $5d^3$ systems (IrF_6 , ReF_6^{-2} , ReCl_6^{-2}). This table is similar to Table 2 except that the linear least square fit was optimized for only the lowest three t_{2g}^3 levels. The predicted energies of the highest two levels are given in parentheses. Note that the highest two levels are calculated as being much higher than observed for IrF_6 and to a lesser extent for ReCl_6^{-2} and ReF_6^{-2} (see text).

a) IrF_6

	$\Gamma_{8g}({}^2T_{1g})$	$\Gamma_{8g}({}^2E_g)$	$\Gamma_{6g}({}^2T_{1g})$	$\Gamma_{7g}({}^2T_{2g})$	$\Gamma_{8g}({}^2T_{2g})$
Observed: (a)	6261	8333	8858	12328	15156
Calculated:	6275	8322	8793	(12922)	(17084)

Parameters: $B = 297$, $C = 1167$, $\zeta_{5d} = 4182$, $10 Dq = 35000$, $3B + C = 2058$.

b) ReF_6^{-2}

Observed:	9080 ^(b)	10130 ^(b)	11160 ^(b)	17390 ^(c)	18670 ^(c)
Calculated:	9080	10130	11160	(17102)	(18046)

Parameters: $B = 792$, $C = 1179$, $\zeta_{5d} = 2745$, $10 Dq = 33000$, $3B + C = 3555$.

c) ReCl_6^{-2}

	$\Gamma_{8g}({}^2T_{1g})$	$\Gamma_{8g}({}^2E_g)$	$\Gamma_{6g}({}^2T_{1g})$	$\Gamma_{7g}({}^2T_{2g})$	$\Gamma_{8g}({}^2T_{2g})$
Observed: (d)	7600 ^(b)	8906	9344	13840	15298
Calculated:	7600	8906	9344	(14704)	(16349)

Parameters: $B = 333$, $C = 1873$, $\zeta_{5d} = 2792$, $10 Dq = 31000$, $3B + C = 2872$.

a) Reference 9.

b) Reference 8.

c) Reference d, Table 2.

d) Reference f, Table 2.

Table 4. a) Energies of the t_{2g}^3 levels of IrF_6 in the gas phase and in various crystals. For the Γ_{8g} levels, which are slightly split by a low-symmetry crystal field, the center of gravity is given.

b) Energies of the t_{2g} levels of ReF_6 in the gas phase and in various crystals. The split Γ_{8g} levels are treated as above.

a) IrF_6

	$\Gamma_{8g} ({}^4A_2)$	$\Gamma_{8g} ({}^2T_{1g})$	$\Gamma_{8g} ({}^2E_g)$	$\Gamma_{6g} ({}^2T_{1g})$	$\Gamma_{7g} ({}^2T_{2g})$	$\Gamma_{8g} ({}^2T_{2g})$
IrF_6 (Vapor) ^(a)	0	6261	8333	8858	12328	15156
Neat IrF_6 (-2.2 K) ^(a)	0	6114	8177	8701	12060	14878
Neat IrF_6 (295 K) ^(b)	0	6188	8256	8779	12177	14947
IrF_6/UF_6 ^(b)	0	6111	8185	8708	12082	14883
IrF_6/WF_6 ^(b)	0	6135	8206	8730	12118	14926
$\text{IrF}_6/\text{MoF}_6$	0	6123 ^(c)	8194 ^(d)	8720 ^(d)	12093 ^(e)	14901 ^(e)

b) ReF_6

	$\Gamma_{8g} ({}^2T_{2g})$	$\Gamma_{7g} ({}^2T_{2g})$
ReF_6 (Vapor) ^(f)	0	5001
ReF_6/UF_6 ^(g)	0	5003
ReF_6/WF_6 ^(g)	0	5001
$\text{ReF}_6/\text{MoF}_6$ ^(g)	0	4997

a) Reference 9.

b) E. R. Bernstein, J. D. Webb, unpublished results.

c) Reference 11.

d) Table 1.

e) Reference 12.

f) J.C.D. Brand, G. L. Goodman, B. Weinstock, J. Mol. Spec. 38, 449 (1971).

g) E. R. Bernstein, G. R. Meredith, J. Chem. Phys. 64, 375 (1976).

Table 5. a) Gas-to-crystal shifts in cm^{-1} ($\Delta\Gamma = \Gamma(\text{crystal}) - \Gamma(\text{gas})$) for mixed and neat crystals of IrF_6 (see Table 4a). The parenthetical numbers represent the shifts as normalized to the smallest shift for a given host.

a) IrF_6

	$\Delta\Gamma_{8g}({}^2T_{1g})$	$\Delta\Gamma_{8g}({}^2E_g)$	$\Delta\Gamma_{8g}({}^2T_{1g})$	$\Delta\Gamma_{7g}({}^2T_{2g})$	$\Delta\Gamma_{8g}({}^2T_{2g})$
MIXED CRYSTALS					
IrF_6/UF_6	-150 (1.01)	-148 (1.00)	-150 (1.01)	-246 (1.66)	-272 (1.84)
IrF_6/WF_6	-126 (1.00)	-127 (1.01)	-128 (1.02)	-210 (1.67)	-230 (1.82)
$\text{IrF}_6/\text{MoF}_6$	-138 (1.00)	-139 (1.01)	-138 (1.00)	-235 (1.70)	-255 (1.85)
NEAT CRYSTALS					
$\text{IrF}_6(-2.2 \text{ K})$	-147 (1.00)	-156 (1.06)	-157 (1.07)	-268 (1.82)	-278 (1.89)
$\text{IrF}_6(295 \text{ K})$	-73 (1.00)	-77 (1.05)	-79 (1.08)	-151 (2.07)	-209 (2.86)

b) Gas-to-crystal shifts for mixed crystals of ReF_6 (see Table 4b).

	$\Delta\Gamma_{7g}({}^2T_{2g})$
ReF_6/UF_6	2
ReF_6/WF_6	0
$\text{ReF}_6/\text{MoF}_6$	3

Table 6. Calculated energies (cm^{-1}) of the upper t_{2g}^3 levels of IrF_6 and the higher t_{2g} level of ReF_6 as a function of $10 Dq$. Full $5d^3 e_g-t_{2g}$ wave functions and configuration interaction are used. The electrostatic and spin-orbit parameters (all in wavenumbers) used for IrF_6 are the following: $B = 297$, $C = 1167$, $\zeta_{5d} = 4182$. The spin-orbit parameter used for ReF_6 is $\zeta_{5d} = 3200$. The parenthetical numbers represent a gas-to-crystal shift if $10 Dq = 35,000 \text{ cm}^{-1}$ represents the gas phase value, while the $10 Dq$ values across the top of the table are taken to represent those in the crystal.

10 Dq	25000	30000	35000	40000	45000	50000
IrF_6						
$\Gamma_{8g}({}^2T_{1g})$	6390 (115)	6324 (49)	6275 (0)	6238 (-37)	6209 (-66)	6185 (-90)
$\Gamma_{8g}({}^2E_g)$	8438 (116)	8370 (48)	8322 (0)	8285 (-37)	8275 (-47)	8234 (-88)
$\Gamma_{6g}({}^2T_{1g})$	9028 (235)	8895 (102)	8793 (0)	8712 (-81)	8646 (-147)	8592 (-201)
$\Gamma_{7g}({}^2T_{2g})$	13096 (174)	13006 (84)	12922 (0)	12849 (-73)	12786 (-136)	12733 (-189)
$\Gamma_{8g}({}^2T_{2g})$	17341 (257)	17205 (121)	17084 (0)	16983 (-101)	16899 (-185)	16829 (-255)
ReF_6						
$\Gamma_{7g}({}^2T_{1g})$	5365 (150)	5278 (63)	5215 (0)	5166 (-49)	5127 (-88)	5096 (-119)

Table 7. Tetragonal d^3 crystal field matrix elements in a strong field-double group O_h^* basis. The matrix elements were obtained by transforming Rahman's (a) tetragonal matrix elements from a single group to a double group basis. ρ and μ are defined by Rahman (a) and in the text. The ordering of the basis functions is that of Runciman and Schroeder (b) since these matrix elements are combined with theirs to obtain the full d^3 matrices. The Γ_6 (O_h^*) and Γ_7 (O_h^*) basis functions are numbered from 22-30, while Γ_8 (O_h^*) are numbered from 1-21. The D_{4h}^* matrix elements are obtained in 2 blocks, Γ_{6g} (D_{4h}^*) and Γ_{7g} (D_{4h}^*). The correlation between O_h^* and D_{4h}^* is such that: $\Gamma_{6g} \rightarrow \Gamma_{6g}$, $\Gamma_{7g} \rightarrow \Gamma_{7g}$, and $\Gamma_{8g} \rightarrow \Gamma_{6g} + \Gamma_{7g}$.

Γ_{6g} (D_{4h}^*): Γ_{8g} (O_h^*) - Γ_{8g} (O_h^*) Sub-block

$E6(3,4) = -\frac{\sqrt{3}}{3} \rho$	$E6(6,8) = -\frac{1}{5} \mu$	$E6(12,12) = \frac{1}{3} \rho + \frac{1}{4} \mu$	$E6(17,17) = -\frac{1}{3} \rho$
$E6(5,5) = -\frac{4}{15} \rho + \frac{1}{5} \mu$	$E6(7,7) = \frac{4}{15} \rho + \frac{1}{5} \mu$	$E6(12,14) = \frac{1}{4} \mu$	$E6(18,18) = -\frac{1}{3} \rho$
$E6(5,6) = \frac{1}{5} \rho - \frac{3}{20} \mu$	$E6(7,8) = -\frac{1}{5} \rho - \frac{3}{20} \mu$	$E6(13,13) = -\frac{1}{3} \rho - \frac{1}{4} \mu$	$E6(18,19) = \frac{1}{2} \mu$
$E6(5,7) = \frac{1}{5} \mu$	$E6(8,8) = -\frac{4}{15} \rho - \frac{1}{5} \mu$	$E6(14,14) = -\frac{1}{3} \rho + \frac{1}{4} \mu$	$E6(19,19) = \frac{1}{3} \rho$
$E6(5,8) = -\frac{3}{20} \mu$	$E6(9,10) = \frac{2}{3} \rho$	$E6(15,15) = \frac{4}{15} \rho$	$E6(19,20) = -\frac{1}{2} \mu$
$E6(6,6) = \frac{4}{15} \rho - \frac{1}{5} \mu$	$E6(11,11) = \frac{1}{3} \rho - \frac{1}{4} \mu$	$E6(15,16) = -\frac{1}{5} \rho$	$E6(20,20) = \frac{1}{3} \rho$
$E6(6,7) = -\frac{3}{20} \mu$	$E6(11,13) = -\frac{1}{4} \mu$	$E6(16,16) = -\frac{4}{15} \rho$	$E6(21,21) = \frac{1}{2} \mu$

Table 7. (continued)

$\Gamma_{6g} (D_{4h}^*): \Gamma_{8g} (0_h^*) - \Gamma_{6g} (0_h^*)$ Sub-block			
$E6(4,22) = \sqrt{\frac{6}{3}} \rho$	$E6(7,23) = -\sqrt{\frac{5}{20}} \mu$	$E6(10,25) = \frac{2}{3} \rho + \frac{1}{2} \mu$	$E6(15,28) = \sqrt{\frac{5}{15}} \rho$
$E6(5,23) = -\sqrt{\frac{5}{15}} \rho + \sqrt{\frac{5}{20}} \mu$	$E6(7,24) = \sqrt{\frac{5}{5}} \rho + \frac{3\sqrt{5}}{20} \mu$	$E6(11,26) = \sqrt{\frac{2}{3}} \rho - \sqrt{\frac{2}{4}} \mu$	$E6(16,28) = \sqrt{\frac{5}{5}} \rho$
$E6(5,24) = -\frac{3\sqrt{5}}{20} \mu$	$E6(8,23) = -\frac{3\sqrt{5}}{20} \mu$	$E6(12,27) = \sqrt{\frac{2}{3}} \rho + \sqrt{\frac{2}{4}} \mu$	$E6(17,29) = -\sqrt{\frac{2}{3}} \rho$
$E6(6,23) = -\sqrt{\frac{5}{5}} \rho + \frac{3\sqrt{5}}{20} \mu$	$E6(8,24) = -\sqrt{\frac{5}{15}} \rho - \sqrt{\frac{5}{20}} \mu$	$E6(13,26) = \sqrt{\frac{2}{4}} \mu$	$E6(18,30) = -\sqrt{\frac{2}{3}} \rho$
$E6(6,24) = \sqrt{\frac{5}{20}} \mu$	$E6(9,25) = -\frac{2}{3} \rho$	$E6(14,27) = -\sqrt{\frac{2}{4}} \mu$	$E6(19,30) = -\sqrt{\frac{2}{2}} \mu$

$\Gamma_{7g} (D_{4h}^*): \Gamma_{8g} (0_h^*) - \Gamma_{8g} (0_h^*)$ Sub-block

$E7(i,j) = -E6(i,j) \quad i, j \leq 21$

Table 7. (continued)

 $\Gamma_{7g} (D_{4h}^*): \Gamma_{8g} (0^*) - \Gamma_{7g} (0^*)$ Sub-block

$E7(3,22) = -\frac{\sqrt{5}}{3} \rho$	$E7(7,24) = -\frac{\sqrt{5}}{15} \rho - \frac{\sqrt{5}}{20} \mu$	$E7(12,27) = \frac{\sqrt{2}}{4} \mu$	$E7(19,29) = -\frac{\sqrt{2}}{3} \rho$
$E7(5,23) = -\frac{\sqrt{5}}{5} \rho + \frac{3\sqrt{5}}{20} \mu$	$E7(8,23) = \frac{\sqrt{5}}{20} \mu$	$E7(13,26) = \frac{\sqrt{2}}{3} \rho + \frac{\sqrt{2}}{4} \mu$	$E7(19,30) = \frac{\sqrt{2}}{2} \mu$
$E7(5,24) = \frac{\sqrt{5}}{20} \mu$	$E7(8,24) = -\frac{\sqrt{5}}{5} \rho - \frac{3\sqrt{5}}{20} \mu$	$E7(14,27) = \frac{\sqrt{2}}{3} \rho - \frac{\sqrt{2}}{4} \mu$	$E7(20,29) = \frac{\sqrt{2}}{2} \mu$
$E7(6,23) = \frac{\sqrt{5}}{15} \rho - \frac{\sqrt{5}}{20} \mu$	$E7(9,25) = -\frac{2}{3} \rho$	$E7(15,28) = \frac{\sqrt{5}}{5} \rho$	$E7(20,30) = -\frac{\sqrt{2}}{3} \rho$
$E7(6,24) = \frac{3\sqrt{5}}{20} \mu$	$E7(10,25) = \frac{2}{3} \rho + \frac{1}{2} \mu$	$E7(16,28) = -\frac{\sqrt{5}}{15} \rho$	
$E7(7,23) = -\frac{3\sqrt{5}}{20} \mu$	$E7(11,26) = -\frac{\sqrt{2}}{4} \mu$	$E7(18,29) = \frac{\sqrt{2}}{2} \mu$	

a) Reference 14.

b) Reference 6.

Table 8. Site splitting of Γ_{8g} levels of IrF_6 - results of a tetragonal crystal field calculation for the t_{2g}^3 levels with the parameters: $B = 340$, $C = 1117$, $\zeta_5 = 3987$, $10 Dq = 35000 \text{ cm}^{-1}$ (a), and tetragonal parameters ρ and μ . These latter parameters are defined in Equations 1 and 2 and are given here in cm^{-1} (see text). The splittings of the Γ_8 states as a function of these parameters is given in cm^{-1} .

ρ	μ	$\Gamma_8 (^4A_2)$	$\Gamma_8 (^2T_{1g})$	$\Gamma_{8g} (^2E_g)$	$\Gamma_8 (^2T_{2g})$
52	0	10	28	0.1	38
52	100	8.7	27	0.1	38
52	500	2.6	25	0.1	37

a) These parameter values were chosen to match the $\text{IrF}_6/\text{MoF}_6$ data with a Jahn-Teller correction of 100 cm^{-1} added to the $\Gamma_{8g} (^2T_{1g})$ experimental energy. However, the results, especially the splitting of the $\Gamma_{8g} (^2E_g)$ level, are not sensitive to the choice of parameters.

Table 9. Onset frequencies (cm^{-1}) of the intense charge-transfer bands in various hexahalides.

	IrF_6 (a)	ReF_6 (a)	ReF_6^{-2} (b)	ReCl_6^{-2} (b)	UF_6 (c)	WF_6 (d)	MoF_6 (d)
σ_{CT}	18500	24000	>35000	21000	24500	60000	50000

a) Reference 2.

b) Reference 8. It is stated in reference e that the near UV bands in ReCl_6^{-2} are ligand field bands rather than charge transfer bands; however, recent work(f) has shown that the original charge transfer assignment(8) is correct.

c) R. S. McDowell, S. W. Rabideau, A. H. Zeltmann, R. T. Paine, J. Chem. Phys. 65, 2707 (1976).

d) R. McDiarmid, J. Mol. Spec. 39, 332 (1971); J. Chem. Phys. 61, 3333 (1974).

e) P. B. Dorain, R. G. Wheeler, J. Chem. Phys. 45, 1172 (1966).

f) J. C. Collingwood, S. B. Piepho, R. W. Schwartz, P. A. Dobosh, J. R. Dickinson, P. N. Schatz, Mol. Phys. 29, 793 (1975).

Table 10. Splittings of Γ_{8g} levels of IrF_6 in various mixed crystals by a low symmetry crystal field, given in wavenumbers. Compare with Table 8.

	$\Gamma_{8g}({}^4A_2)$	$\Gamma_{8g}({}^2T_{1g})$	$\Gamma_{8g}({}^2E_g)$	$\Gamma_{8g}({}^2T_{2g})$
IrF_6/UF_6 ^(a)	10.0	61.9	53.0	66.4
IrF_6/WF_6 ^(a)	5.7	38.6	34.8	46.3
$\text{IrF}_6/\text{MoF}_6$	5.2 ^(b)	34.7 ^(c)	30.6 ^(d)	42.1 ^(b)

a) E. R. Bernstein and J. D. Webb, unpublished results.

b) Reference 12.

c) Reference 12.

d) Table 1.

Figure 1.

Origin of the Γ_{8g} (2E_g) electronic state of $\text{IrF}_6/\text{MoF}_6$. The origin is split by a low symmetry crystal field; see Figure 2 for verification of this assignment.

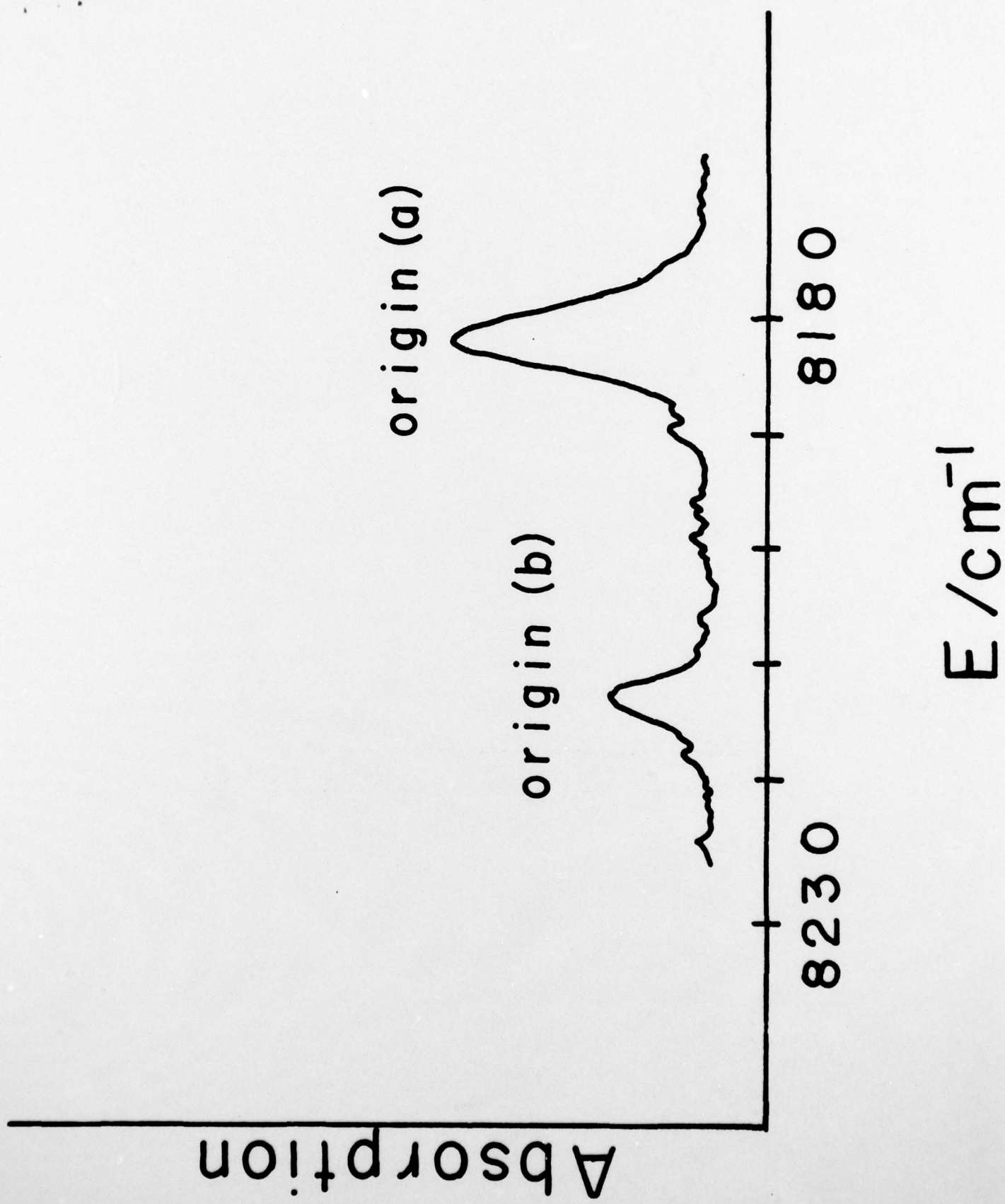
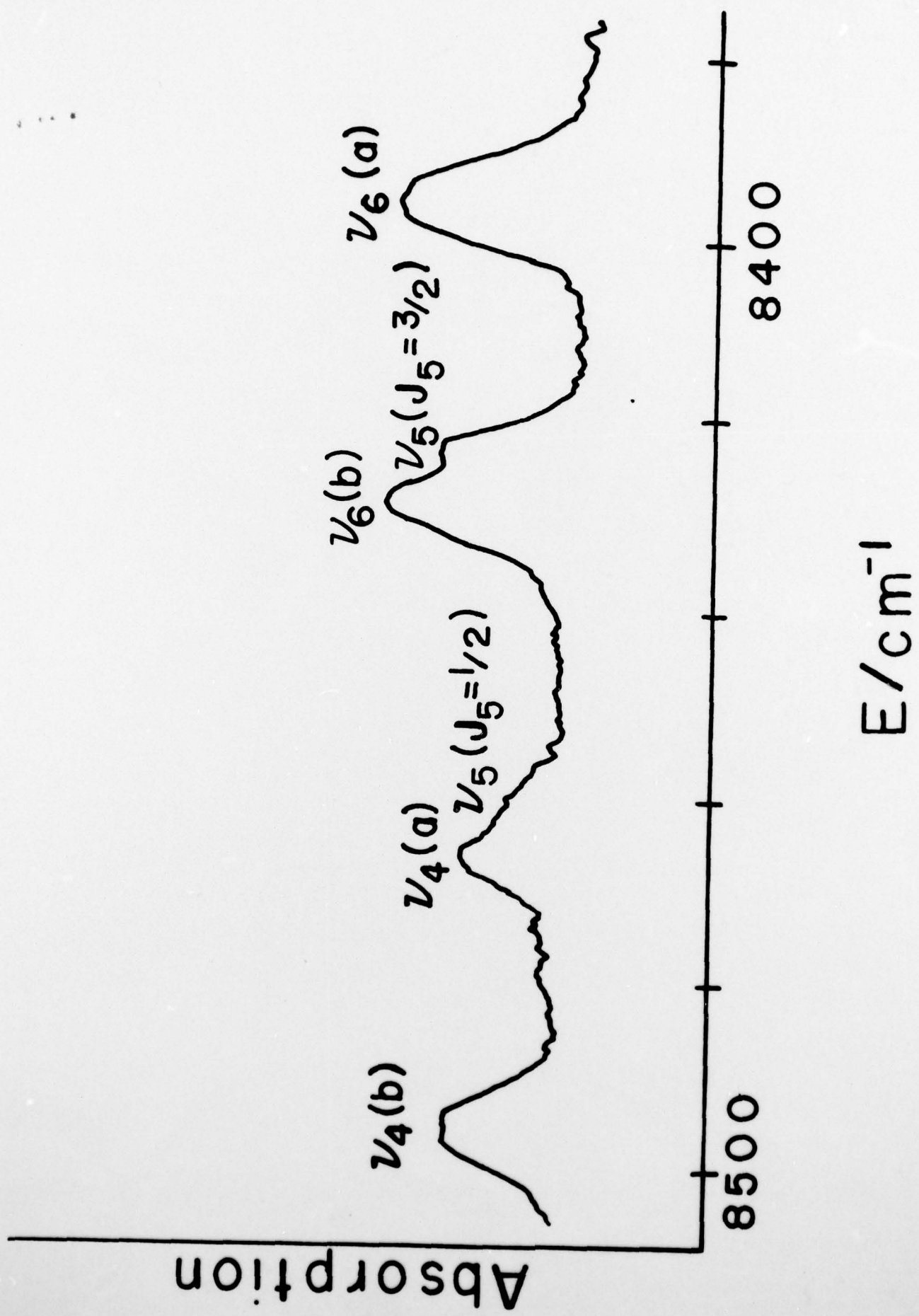


Figure 2.

Vibrational bending region of the Γ_{8g} (2E_g) electronic state of $\text{IrF}_6/\text{MoF}_6$. Note that the $\sim 30 \text{ cm}^{-1}$ spacing of the $\nu_6(t_{2u})$ and $\nu_4(t_{1u})$ components matches the origin splitting, verifying that the observed lines are due to a low symmetry crystal field splitting. A small linear Jahn-Teller splitting of $\nu_5(t_{2g})$ is also apparent.



TECHNICAL REPORT DISTRIBUTION LIST

<u>No. Copies</u>		<u>No. Copies</u>
	Office of Naval Research Arlington, Virginia 22217 Attn: Code 472	2
	Office of Naval Research Arlington, Virginia 22217 Attn: Code 102IP 1	6
	ONR Branch Office 536 S. Clark Street Chicago, Illinois 60605 Attn: Dr. Jerry Smith	1
	ONR Branch Office 715 Broadway New York, New York 10003 Attn: Scientific Dept.	1
	ONR Branch Office 1030 East Green Street Pasadena, California 91106 Attn: Dr. R. J. Marcus	1
	ONR Branch Office 760 Market Street, Rm. 447 San Francisco, California 94102 Attn: Dr. P. A. Miller	1
	ONR Branch Office 495 Summer Street Boston, Massachusetts 02210 Attn: Dr. L. H. Peebles	1
	Director, Naval Research Laboratory Washington, D.C. 20390 Attn: Code 6100	1
	The Asst. Secretary of the Navy (R&D) Department of the Navy Room 4E736, Pentagon Washington, D.C. 20350	1
	Commander, Naval Air Systems Command Department of the Navy Washington, D.C. 20360 Attn: Code 310C (H. Rosenwasser)	1
	Defense Documentation Center Building 5, Cameron Station Alexandria, Virginia 22314	12
	U.S. Army Research Office P.O. Box 12211 Research Triangle Park, N.C. 27709 Attn: CRD-AA-IP	1
	Naval Ocean Systems Center San Diego, California 92152 Attn: Mr. Joe McCartney	1
	Naval Weapons Center China Lake, California 93555 Attn: Head, Chemistry Division	1
	Naval Civil Engineering Laboratory Port Hueneme, California 93041 Attn: Mr. W. S. Haynes	1
	Professor O. Heinz Department of Physics & Chemistry Naval Postgraduate School Monterey, California 93940	1
	Dr. A. L. Slafkosky Scientific Advisor Commandant of the Marine Corps (Code RD-1) Washington, D.C. 20380	1
	Office of Naval Research Arlington, Virginia 22217 Attn: Dr. Richard S. Miller	1

TECHNICAL REPORT DISTRIBUTION LIST

	<u>No. Copies</u>		<u>No. Copies</u>
Dr. M. A. El-Sayed University of California Department of Chemistry Los Angeles, California 90024	1	Dr. G. B. Schuster University of Illinois Chemistry Department Urbana, Illinois 61801	1
Dr. M. W. Windsor Washington State University Department of Chemistry Pullman, Washington 99163	1	Dr. E. M. Eyring University of Utah Department of Chemistry Salt Lake City, Utah	1
Dr. E. R. Bernstein Colorado State University Department of Chemistry Fort Collins, Colorado 80521	1	Dr. A. Adamson University of Southern California Department of Chemistry Los Angeles, California 90007	1
Dr. C. A. Heller Naval Weapons Center Code 6059 China Lake, California 93555	1	Dr. M. S. Wrighton Massachusetts Institute of Technology Department of Chemistry Cambridge, Massachusetts 02139	1
Dr. M. H. Chisholm Princeton University Department of Chemistry Princeton, New Jersey 08540	1	Dr. M. Rauhut American Cyanamid Company Chemical Research Division Bound Brook, New Jersey 08805	1
Dr. J. R. MacDonald Naval Research Laboratory Chemistry Division Code 6110 Washington, D.C. 20375	1		